Direct TEM observation of α/γ interface migration during cyclic partial phase transformations at intercritical temperatures in an Fe-0.1C −0.5Mn alloy

Nutter, J.; Farahani, H.; Rainforth, W. M.; van der Zwaag, S.

Important note
To cite this publication, please use the final published version (if applicable).
Please check the document version above.

Full length article

Direct TEM observation of α/γ interface migration during cyclic partial phase transformations at intercritical temperatures in an Fe-0.1C −0.5Mn alloy

J. Nutter [a, *], H. Farahani [b], W.M. Rainforth [a], S. van der Zwaag [b]

[a] Department of Materials Science and Engineering, University of Sheffield, Western Bank, Sheffield, S10 2TN, United Kingdom
[b] Faculty of Aerospace Engineering, Delft University of Technology, Kluyverweg 1, 2629 HS, Delft, the Netherlands

ABSTRACT

The kinetic behaviour of austenite/ferrite interfaces in a low carbon − 0.5 mass% Mn containing steel during Cyclic Partial Phase Transformation (CPPT) experiments has been investigated using hot stage Transmission Electron Microscopy (TEM). Individual interfaces were observed to display behaviour typical of CPPT experiments as recorded in macroscopic dilatometry experiments and demonstrated i) the "normal", ii) inverse transformations and iii) a stagnant stage in which the interface migrates at a very low velocity as a result of the interface passing through a Mn enriched zone due to the preceding transformation. The length of the stagnant stage determined from the TEM observations shows excellent agreement with that measured from dilatometry and kinetic modelling, whilst the distance migrated from the interface shows some disparities which are primarily attributed to differences in assumptions about grain geometry and nucleation. No special interface features were observed when the interface changed direction and passed through the previously Mn-enriched zones. General observations on the interaction of the transformation interface with microstructural features are also reported.

© 2019 Acta Materialia Inc. Published by Elsevier Ltd. All rights reserved.

1. Introduction

The solid-state phase transformations which occur during thermomechanical processing of relatively lean construction and automotive steels are key to the production of different microstructures and therefore different mechanical properties in the final product [1,2]. Hence understanding the kinetics of these transformations has attracted significant research interest for many decades [3−8]. The nucleation and growth of ferrite (α-phase) from the parent austenite (γ-phase) is a key transformation to understanding phase transformations in steels, with the actual growth kinetics found to be intermediate between two limiting cases − diffusion controlled and interface controlled growth, with the rate limiting factor being the diffusion of alloying elements away from the transformation interface and the intrinsic mobility of the interface itself respectively [9−11]. The actual rate of interface migration is a function of the temperature and the transient enrichment of substitutional alloying elements at the moving austenite-ferrite interfaces [3].

Since in the usual isothermal and isochronal transformation studies the effects of (continued) nucleation and (simultaneous) growth cannot be separated and the effect of element partitioning on the interface mobility cannot be determined accurately, recently the concept of cyclic partial phase transformations (CPPT) has been used to investigate partitioning phase transformations in Fe−C-M and Fe−C−Mn-X alloys using modelling and experiments [12−20]. During a cyclic partial phase transformation experiment the temperature is cycled between two temperatures, T_1 and T_2, both within the α+γ phase region [14]. Using this approach, the effect of nucleation, which is difficult to measure experimentally [14], can be excluded from an analysis of the kinetics as the transformation only progresses through the migration of already existing interfaces [13,21]. Secondly, in a CPPT experiment it is much easier to unambiguously allocate the interface kinetics to the local interface conditions present, which in itself is a function not only of the steel composition (in particular the Mn concentration as Mn has a high partitioning coefficient and can affect the effective interface mobility significantly [15]) and also of the thermal history.

While the results of conventional dilatometry during CPPT in terms of interface behaviour and kinetics can be analysed based on

relatively simple and undisputed assumptions regarding the initial and transient grain structures, and assuming all grains behave more or less identically, understanding the mechanisms responsible for the transformation stages can be informed by direct observation of the motion of individual interfaces during the various stages of the CPPT transformation and recording the changes in interface velocity and interface character (if any).

Previously, hot stage TEM experiments have been used to successfully observe transformation behaviour in steels during the austenite to ferrite or ferrite to austenite [22—25], austenite to bainite [26,27] and austenite to pearlite transformations [28] under continuous cooling or heating or isothermal conditions. Interfaces were observed to continuously change in character (from clearly incoherent to likely to be coherent) along the moving interface and to interact with microstructural features and suggested that interfacial structure may influence the mobility of the interface, however, in the previous TEM experiments the interface motion observations were only qualitative linked to the macroscopically determined transformation kinetics.

Adapting CPPT experiments for in situ hot stage TEM experiments allows the direct observation of the behaviour of individual α/γ interfaces during cyclic heat treatment. In particular, this makes it possible to investigate in greater detail the interface behaviour and morphology immediately before, during and after the stagnant stage, this being the most discriminating feature in the CPPT concept and the feature affected most strongly by local substitutional element concentrations.

2. Experimental

2.1. Materials examined

The composition of the steel used in this study was Fe-0.0848C-0.47Mn (mass%), with the full composition given in Table 1 below. This steel was selected as it has been used most extensively in the original and later CPPT experiments and showed clear manifestations of the normal, stagnant and inverse transformations under a wide range of cycling conditions [16—18]. The initial microstructure consisted of a mixture of allotriomorphic, Widmanstätten and bainitic ferrite. Machined 5 mm × 10 mm cylindrical specimens suitable for dilatometry were sectioned along the cylinder axis and mechanically thinned to 100 μm. 3 mm discs were punched out from this material and electropolished using a Struers TenuPol-5 electropolishing unit at −40 °C with a 5% Perchloric Acid, 35% 2-Butoxyethanol, 60% Methanol Solution. Specimens with a smooth central perforation and large electron transparent region were selected for use in the TEM experiments.

2.2. Dilatometry

To guide the setting the right temperature and cooling and heating conditions for the in-situ transformations in the TEM and to link the observations of individual interfaces to macroscopic behaviour, companion dilatometry experiments were performed. To this aim, cylindrical specimens were heat treated using a DIL 805D dilatometer, in vacuum. The temperature difference across the specimen was monitored by spot welding thermal couples at the end and centre of the sample. For reliable and accurate measurements, only those measurements for which the temperature difference between the two thermocouples was less than 3 °C were used.

2.3. In situ hot stage TEM

Hot stage TEM was carried out in a JEOL JEM 3010 UHR TEM operated at 300 kV, with a LaB_6 filament, in spot size 1. The hot stage was a GATAN model 628 single tilt heating holder, with a model 628.09 J water re-circulator. The heat treatment was programmed using Python with the PySerial library. This used the SMART heating mode to adjust the temperature at regular intervals, whilst simultaneously collecting the measured temperature from the holder. A typical example of the thermal cycle yielding the most informative TEM observations is shown in Fig. 1 below. The heating and cooling rates were ±8.6 °C/min, and T_1 and T_2 were selected as 790 °C and 840 °C respectively. Extensive preliminary experiments were conducted to determine the mismatch between the actual sample temperature in the field of view and the temperature setting of the specimen holder [29]. These indicated that there was a 130 °C temperature difference between the specimen temperature and that measured by the thermocouple. However, since the stagnant stage length is dependent on heating/cooling rate, we are confident that the relative temperatures measured during successful thermal cycling are accurate, due to the close match (discussed below) between the TEM observations and bulk experiment.

The transient TEM images from which the interface migration was derived were recorded using a TVIPS camera attached to the JEOL 3010 operating with a 100 ms exposure time. Recordings were started some time before the expected occurrence of the first step in the transformation and were continued for three heating and cooling (T_1-T_2-T_1) cycles or as long the interface could be followed. If necessary, the sample was repositioned with respect to the beam in order to keep track of the moving interface or to shift to relevant features in its vicinity. To have the right balance between resolution and tracking of the moving interface a low magnification of 4,000 times was applied resulting in a field of view of 5.8 × 5.8 μm. The uninterrupted recording times ranged from 40 to 60 min. A total of five specimens underwent the heat treatment. Three specimens were successfully cycled in the two-phase region, whilst the two remaining specimens became fully austenitic in the electron

Table 1
Table of composition of the materials used in the TEM and dilatometry experiments (all in mass%).

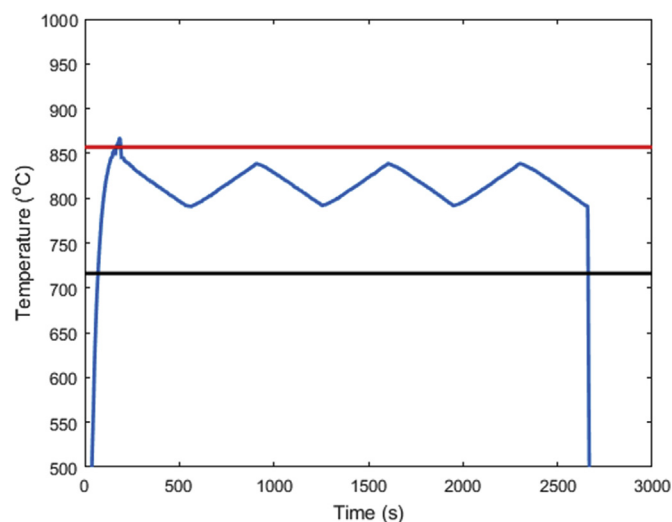| C	Mn	Si	Al	B	S, N	O	Fe
0.848	0.47	0.03	0.02	<0.0003	<0.001	0.0017	Balance

Fig. 1. Temperature against time for the imposed heat treatment, with the start and finish temperatures of the two-phase region, determined using Thermo-Calc indicated.

transparent region on heating to T_2 and these latter observations were deemed invalid as there must have been a clear mis-recording of the actual specimen temperature, probably as a result of non-representative thermal contact between the holder and the sample.

2.4. Video analysis

The two phases of interest, austenite and ferrite, were distinguished both during TEM operation and from analysis of the video after the thermal treatment. To determine the phase present on either side of the interface in a more objective manner rapid selected area electron diffraction measurements were made at relevant stages of the thermal cycle and these were recorded on the video as well. After the experiment, still frames from the video were sampled at intervals with a particular focus on extracting the position of the interface. Automatic alignment of these frames was carried out using the *Linear Stack alignment with SIFT* plugin for the FIJI is Just ImageJ (FIJI) software and manually with the GNU Image Manipulation Program (GIMP) using any immobile feature in the frames as a reference. Interface velocities were determined by measuring the distance travelled more or less normal to the interface migration between frames. Where appropriate this was done for a single observed section of interface at regular intervals of 500 nm and these measurements were used to calculate standard errors.

2.5. Kinetic modelling

Kinetic modelling was performed using DICTRA [30] with the MOBFE2 and TCFE8 databases. A composition of Fe-0.0848-0.47Mn was used and the heat treatment was selected to match the T_1 and T_2 temperatures and the heating/cooling rates achieved in the TEM experiments. In the calculations two austenite region sizes of 25 or 40 μm were used, representing austenite grain sizes of 50 and 80 μm respectively.

3. Results

3.1. Dilatometry and kinetic modelling

Fig. 2 shows the length change against temperature for during thermal cycling using dilatometry. Characteristic features of CPPT experiments, the inverse transformation and stagnant stage [12,13], as well as the normal transformation are visible and marked in the curves of Fig. 2(a).

A first approximation of the ferrite volume fraction against temperature is shown in Fig. 2(b). This was obtained using the Lever rule. Some caution is necessary interpreting the resulting estimates for the ferrite fraction because the steel is a ternary alloy (i.e. theoretically the Lever rule does not apply) and because the curve is not a closed loop with some transformation plasticity visible during thermal cycling. This volume fraction was used to estimate the interface position and velocity under assumed cubic and spherical geometries as shown in Fig. 2(c–f). The velocity is related to the change in volume fraction by equation (1) [31–34]:

$$df_\alpha/dt = 3(N^*g)^{1/3}(1-f_\alpha^2)v_\alpha arctanh^{2/3}(f_\alpha) \qquad (1)$$

Where N^* is the nuclei density (based on a ferrite grain size of 40 ± 2.2 μm, determined using the standard linear intercept method), g is a geometry factor (g = 1 for cubic and g = 4π/3 for spherical geometry), v_α is the interface velocity and f_α ferrite volume fraction.

Fig. 3 presents the results of DICTRA simulations given the same applied heat treatment. The predicted migration distances with

25 μm and 40 μm austenite grain size are 6.3 and 8.7 μm respectively. These values are intermediate between the estimated 5.6 and 9.0 μm based on interpreting the dilatometer data using a spherical and cubic grain shape estimate.

3.2. TEM observations

Fig. 4(a) and (b) shows the interface position and interface velocity against temperature for the most complete set of interface observations presented in this paper, which are representative of the other, less complete, observations of interface motion across multiple cycles and specimens, with a total of 4 interfaces followed. The presence of the inverse transformation and stagnant stage are clearly apparent in the curve. The total migration distance by interface 2 over the course of the cycle is 19.4 μm, with the average stagnant stage length across all three cycles estimated to be 15 °C (119 s) during cooling and 16 °C (127 s) during heating.

The interface velocity behaviour differed on heating and cooling. During heating there was a sustained increase in velocity during the normal transformation. Although the maximum measured velocity of 700 nms^{-1} occurred at 834 °C, this was associated with the rapid movement of a migrating triple boundary. Measurements of this kind are relatively localised and not necessarily representative of the behaviour of all existing interfaces and are likely to be averaged out when using techniques such as dilatometry. Therefore, the assumed peak for the comparison with bulk data is considered to be at the maximum temperature of the cycle, 838 °C, and to have a value of 300 nms^{-1}. Averaged across 3 cycles the peak velocity was 220 nms^{-1} (with a standard deviation of 70 nm) occurring at 838 °C.

On cooling there was a rapid acceleration of the interface, reaching a peak velocity of 500 nm^{-1} at ~814 °C. Continued cooling lead to a sustained decrease in interface velocity until the minimum temperature of the cycle, 791 °C, was reached. This behaviour was also found for other cycles/interfaces, as shown in Fig. 4(c), where it is compared with the velocity estimated from dilatometry (assuming cubic geometry) and shows good agreement in the peak temperature between TEM and bulk observations. The same peak velocity was measured for another interface which could be tracked successfully during this stage of the transformation.

The interface was captured during the normal and inverse transformations as well as during the stagnant stage. One feature of the interfaces under observation was that there was sometimes a tendency for interfaces between an adjacent ferrite and austenite grain to become segmented. Segmentation is used to describe observations for which the interface between a single austenite and a single ferrite grain displayed distinct regions of differing morphology, i.e. the interface between two grains could therefore display both straight and curved morphologies at different points along its length. This was most commonly seen when there were large numbers of twins in the austenite and was particularly pronounced when the twin boundaries intersected with the austenite-ferrite interface. Segmentation of this type can be seen in Fig. 7(a) where the twin boundary intersects the interface (blue arrow) and separates curved and straight segments of α/γ interface.

During the normal transformation stage, when the migration is relatively rapid, the interface morphology was observed to evolve continuously with the interface shifting between a straight, curved or a wave-like structure. In contrast, the interface displayed a more stable morphology during the stagnant stage. During this period the observed morphology was typically straighter or more monotonically curved. Fig. 5 shows a montage of the austenite-ferrite interface at the end of the stagnant stage and immediately after the start of the normal transformation. The predominantly (but not perfectly) straight interface became visibly more wavelike as
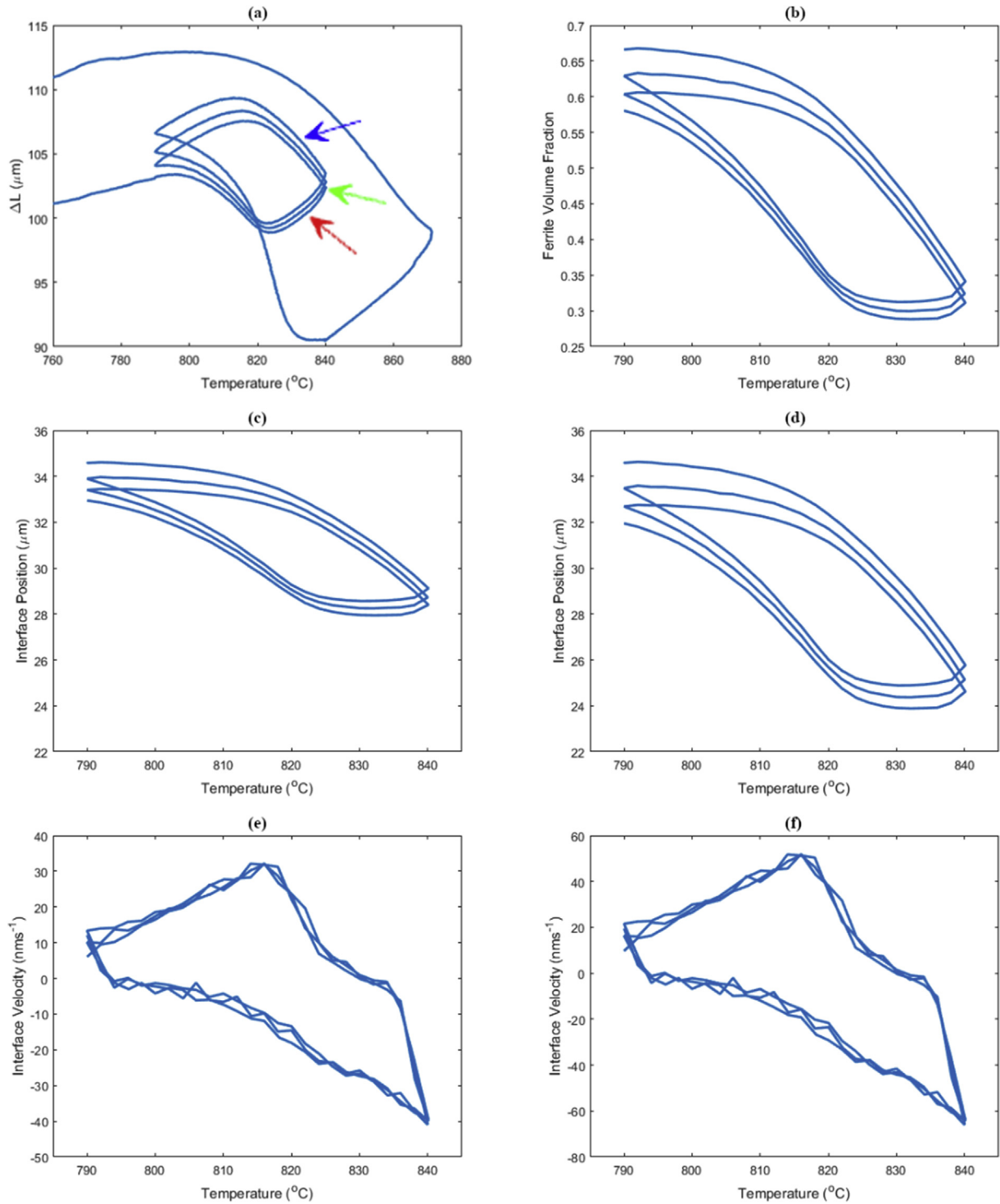
Fig. 2. (a) Length change against temperature during thermal cycling, with the normal and inverse transformation and stagnant stage indicated with blue, green and red arrows respectively, (b) Ferrite volume fraction against temperature, (c) Interface position against temperature assuming spherical geometry, (d) Interface position against temperature assuming cubic geometry, (e) Interface velocity against temperature assuming spherical geometry and (f) Interface velocity against temperature assuming spherical geometry. The interface velocity is negative for the ferrite to austenite transformation. (For interpretation of the references to colour in this figure legend, the reader is referred to the Web version of this article.)

stagnant stage ended and the normal ferrite to austenite transformation commenced.

During the so-called stagnant stage, the interface was not observed to become completely stationary for any significant length of time. Instead, the interface continued to migrate slowly,

and during cooling the migration direction reversed, over the course of the stagnant stage. During the stagnant stage the total distance travelled by the interface plotted in Fig. 4(a) was 0.5 and 1.1 μm respectively for heating and cooling respectively. Averaged across the three cycles, the migration distance was 0.8 μm for
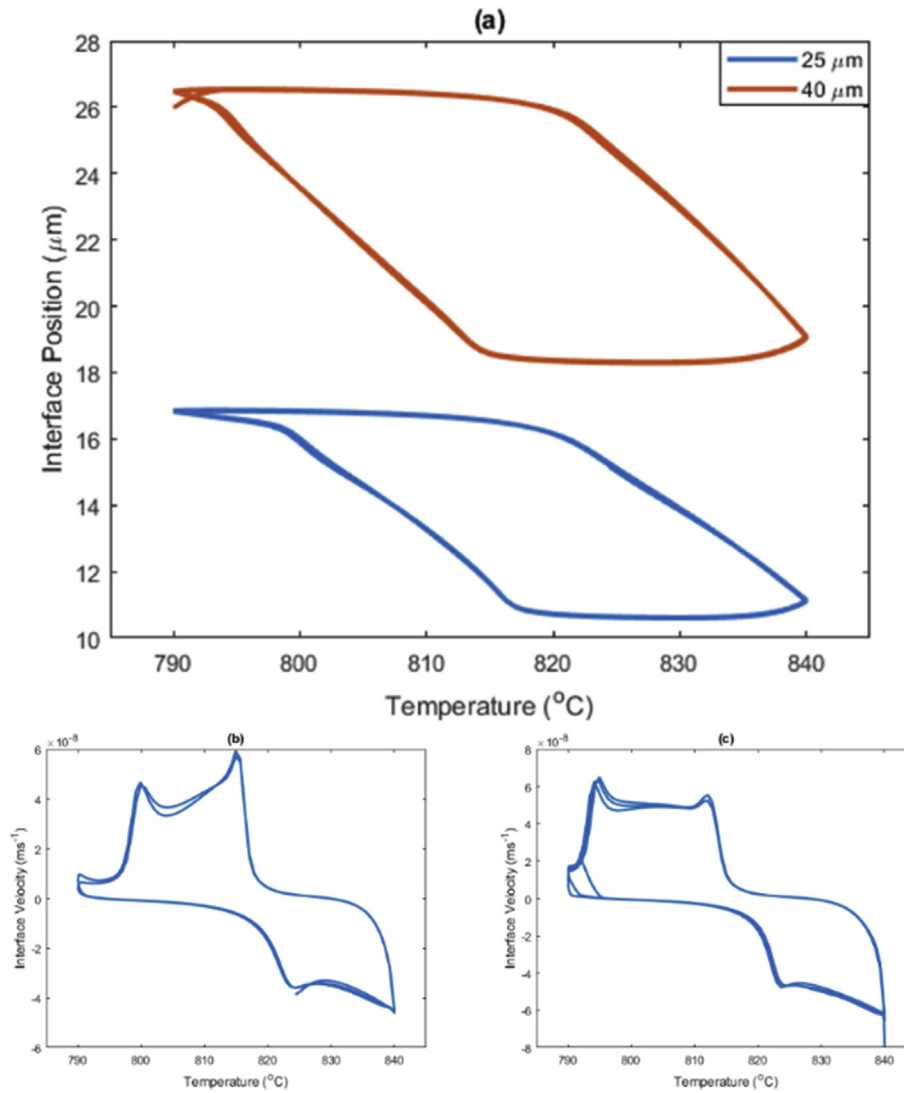
Fig. 3. Predicted interface position against temperature for a 25 μm austenite region and a 40 μm austenite region.

heating and 1.0 μm for cooling. For the interface plotted in Fig. 4(a) the interface migration reversed slightly during cooling so the difference in position between the start and end of the stagnant stage was only 0.2 μm.

More generally, the observations showed that where the position could be correlated across cycles or part of the cycle, the interface occupied approximately (but not exactly) the same locations at the temperatures corresponding to the start of the inverse transformation and the start and end of the stagnant stage. This indicates that there was reasonably good reversibility of the interface across cycles, as has also been deduced on the basis of dilatometric data [17,18] and lower resolution Scanning Laser Confocal experiments [19]. There were some broad similarities in interfacial structure between cycles with the differences primarily attributable to either differences in the location and density of twin boundaries near the interface in the austenite grain or the differences at points were multiple grains of the growing phase met. This is illustrated in Fig. 6 which shows the same length of the interface at equivalent stages of the cycle (in this case, the start of the normal austenite to ferrite transformation) for all three cycles. The curvature of the interface can be seen to be inverted in 6(a) compared to 6(b) and 6(c) due to the presence of twin boundaries behind the interface.

In Fig. 7, part of the ferrite to austenite transformation is shown. Several features of the observed migrating interface are illustrated here. First, as noted above, the austenite grain $\gamma 1$ contains a twin boundary which intersects with the interface as in Fig. 7(a). There is an apparent change in the morphology of the interface at this point with a smoothly curved upper section of the interface clearly distinguishable from the straight section on the lower left side. As the interface migrated, grain $\gamma 2$ grew only slowly (potentially due to shape constraints), resulting in the elimination of the interface between $\gamma 2$ and $\alpha 1$ due to the growth of the adjacent austenite grains. Another noteworthy feature of the behaviour was the changes to the grain boundary topology between the ferrite grains, $\alpha 1$ and $\alpha 2$. Between Fig. 7(a) and (b) the migration of the $\alpha 2$-$\gamma 3$ interface appeared to induce an abrupt change in the curvature of the boundary in the region immediately ahead of the transformation interface. It was not uncommon to observe changing grain boundary structure ahead of, or behind, the α-γ interface during thermal cycling. In cases where a migrating triple point was observed, competition was seen between the two grains of the growing phase, resulting in the lateral displacement of the triple point and the rapid movement of incoherent grain boundaries to
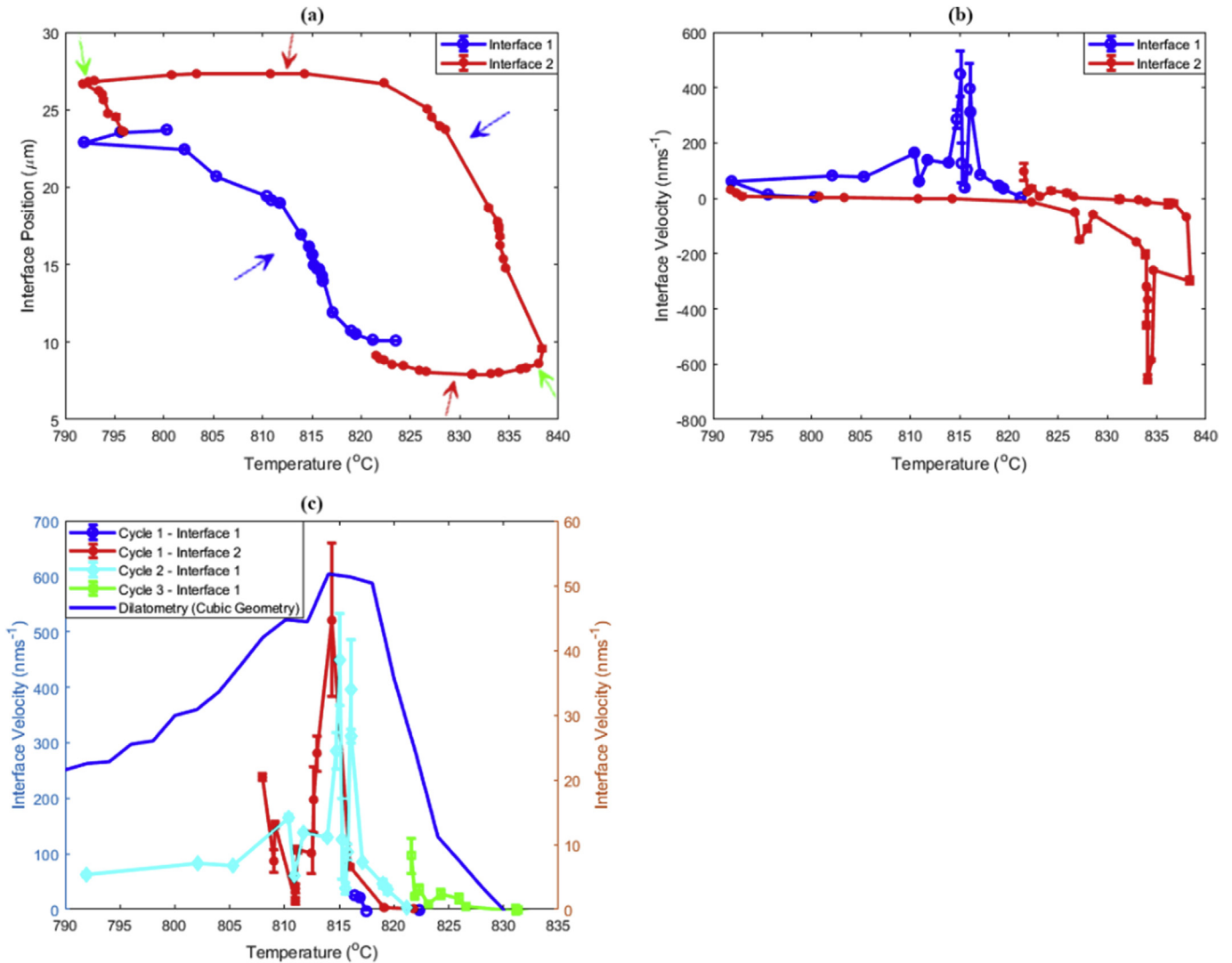
Fig. 4. (a) Interface position against temperature, (b) Interface velocity against temperature as determined for the TEM observations and (c) Interface velocity against temperature for the austenite to ferrite transformation comparing the TEM observations (left hand axis) and dilatometry (right hand axis). The interface velocity is classified as negative for the ferrite to austenite transformation.

accommodate this displacement. At the end of the illustrated period, all of the four remaining grains (two austenite and two ferrite) formed a single junction, which was only maintained for a short period of time.

One unusual aspect of the migration behaviour, intrinsically not detectable from dilatometry data, was localised acceleration of the interface when two interfaces came into close proximity. An example of this process is shown in Fig. 7, where the acceleration rapidly eliminated the remaining ferrite with a zip-like motion. The phenomenon of localised acceleration of interfaces for meeting interfaces has also been observed in recent EBSD experiments [35], however, in this case, the curvature of the interface may have also influenced the behaviour.

Dislocations were observed in the ferrite during interface migration and typically were observed to migrate towards and annihilate with both the α/γ interface and nearby grain boundaries. In general, freshly emitted or pre-existing dislocations were not observed in the austenite grains during thermal cycling. However, this may not indicate the absence of dislocations in the austenite, only that they were not visible under prevailing contrast conditions.

Other dislocation behaviours were also observed. On one occasion dislocations which had been moving ahead of the interface were seen to coalesce and form a structure similar to a low angle boundary in what had previously been a single ferrite grain. This process is shown in Fig. 8.

4. Discussion

The transformation behaviour during a CPPT treatments on a Fe-0.1C-0.5Mn as derived from dilatometric results was almost perfectly reproduced in the in-situ TEM observations of individual moving interfaces and the distinct transformation stages associated with CPPT heat treatments could be identified. On initial cooling the expected, normal transformation from austenite to ferrite was observed. Immediately after reaching the lower T_1 temperature, when heating of the specimen began, the austenite to ferrite transformation was observed to continue for a short time — the so-called inverse transformation. Subsequently, there was a period in which the interface moved only slowly, without ever becoming completely static, which continued on heating, and this corresponds to the stagnant stage identified from dilatometry. The same
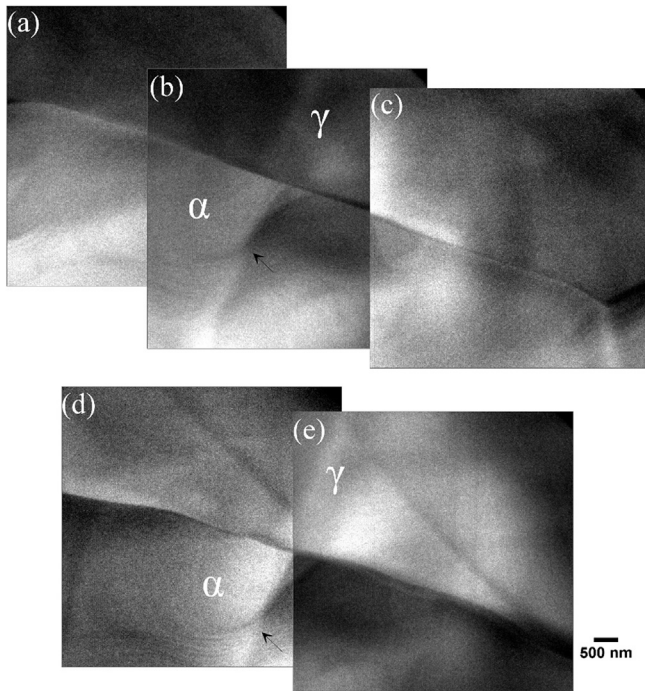
Fig. 5. Composite of bright field TEM images of the interface at (a–c) the end of the stagnant stage (814 °C) and (d–e) after the normal transformation had begun (822 °C). Black arrow indicates features immobile between (b) and (d).

process can be observed for the ferrite to austenite transformation. This further confirms the results of Chen et al. [17,19] that distinctive CPPT behaviour is the result of the behaviour of individual interfaces. There is good almost quantitative agreement between the behaviour of the interface in the TEM and that derived from dilatometry.

Chen et al. [15] estimated the effect of nominal Mn concentration on the duration of the stagnant stage as 35 °C per mass% Mn, by modelling the behaviour of Fe-0.02C-XMN (X = 0.1, 0.2, 0.3) during cyclic partial phase transformations at a heating and cooling rate of 10 °C/min, close to that used in the present experiments. For a 0.5Mn steel this would correspond to a stagnant stage of 17.5 °C. Using the data of Chen et al. to adjust for the different heating and cooling rates (10 °C/min against 8.6 °C/min) the present experiments would be expected to exhibit a stagnant stage of approximately 16 °C. This is in surprisingly good agreement (the deviation being <1 °C) for both stagnant stages as measured in TEM and indicates that similar conditions prevail at the interface in each case. This level of agreement (and that of the good match in the temperature at which the peak velocity during the austenite to ferrite transformation occurred) provides a good indication that interfacial conditions are sufficiently similar in both the TEM experiment and the bulk dilatometry experiments.

During the normal transformations the interface displayed a (relatively) rapidly evolving morphology. The interface often shifted between a straight, curved or wave-like morphology. In the first two cases the migration was smooth, with little change in the shape of the interface. However, when the morphology became wavelike, the interface motion appeared to be undulating with a less stable interface shape. Overall, parts of the interface could be seen to switch between these competing morphologies over the course of the transformation.

The evolution of the morphology also displayed a long-term trend over the course of a single T2-T1-T2 cycle. On cooling, the stagnant stage was characterised by the slow migration of the

boundary accompanied by the reshaping of the interface, which had the effect of inverting the curvature of the interface. In the case of the stagnant stage on heating the inversion of this curvature did not occur until the ferrite to austenite transformation had commenced. In both cases, the interface became more irregular when the normal transformation commenced, displaying the dynamic behaviour outlined above. As the temperature approached the T1 or T2 temperature, the interface became more regular, becoming straighter or smoothly curved, which continued into the inverse transformation.

The interfacial mode switching during the normal transformation are similar to those of Onink et al. [22] in a high purity Fe–C alloy isothermally transformed between 710 and 770 °C. In this case interfaces were also found to vary between curved and nearly straight morphologies and interfaces were also found to undergo segmentation. Since this phenomenon was observed in transformations of both Fe–C–Mn and Fe–C steels, the mode switching during the movement of an interface is considered to be intrinsic rather than due to minute local Mn concentration variations. In the current TEM observations only the actual rate of migration of the interface can be measured, making it difficult to distinguish the contributions of the interface mobility and the driving force. However, since the driving force arises from thermodynamic considerations (temperature and local composition) it is likely that the driving force remains homogeneous along the interface and consequently that the interface mobility is the parameter which varies locally. Many studies of the mobility of grain boundaries [36,37] have shown that boundaries possess different mobilities for different orientations. Therefore, instead of maintaining a particular interface topology along its full length, the interface aims to maximise the overall rate of transformation by progressing faster in regions of relatively high mobility, and slower in regions where mobility is relatively low.

The origin of this friction is the intrinsic resistance to migration which applies even on interfaces in pure metals [38]. Smooth, gently curved interfaces were also observed in Fe–C–Mo steels by Purdy [23] alongside a small number of facetted interfaces. Observations on interstitial free steels using HT-CLSM [39] also found curved α/γ transformation interfaces, and interfaces containing a mixture of smooth and jagged regions.

The observations of local acceleration when two boundaries are in proximity and migrating triple points shows complex interface behaviour. The localised zip-like acceleration may be due to the overall reduction in interfacial energy by replacing two α/γ interfaces with a single γ/γ grain boundary. Studies calculating the grain boundary energy for α-Fe using molecular dynamics indicate that the energy, $\sigma_{\alpha\alpha}$, for $\langle 100 \rangle$ symmetric tilt grain boundaries is up to 1.2 J m^{-2} [40,41]. This is comparable to estimates of the austenite grain boundary energy in low carbon steels at 1000 °C of 1.0–1.3 J m^{-2} [42]. Embedded atom model simulations indicate that the α/γ interfacial energy, $\sigma_{\alpha\gamma}$, is approximately 0.8 J m^{-2} [43]. This indicates that the zip-like acceleration could, in fact, lead to a reduction in the total interfacial energy as $2\sigma_{\alpha\gamma} > \sigma_{\gamma\gamma}$. Furthermore, it shows that neighbouring interfaces, as observed in TEM, also influence the behaviour in ways not necessarily accounted for by traditional models. The observation of accelerated interface motion is against the conventional notion of soft impingement due to overlapping of carbon gradients or hard impingement due to ferrite interfaces meeting. The sample volume affected by the acceleration effect upon grain impingement is, however, too small to be detectable with macroscopic techniques such as dilatometry.

As expected, the agreement between the behaviour was quantitatively less perfect for the interface velocities and the change in position compared to the very nice agreement in stagnant stage length. For the austenite to ferrite transformation the TEM derived
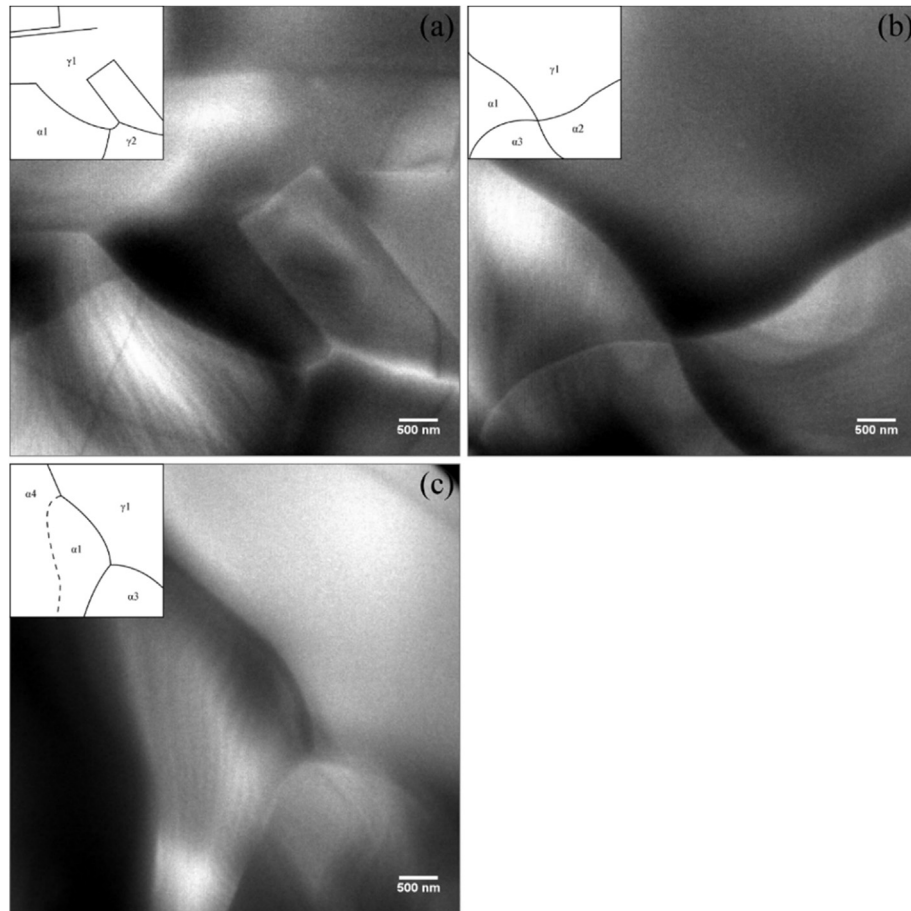
Fig. 6. Bright field TEM of the interface at the beginning of the normal austenite to ferrite transformation for each cycle (a) at 1065.7 s, with the presence of a complex twin structure behind the interface (820°C) (b) 1749.1 s (821°C) and (c) 2435.1 s (823°C).

peak velocities were a factor of 11 times higher than those estimated from dilatometry and applying a very simple averaging technique based on spherical grain morphology. The TEM peak velocities were a factor of 5 times higher than the dilatometry derived peak velocity for the ferrite to austenite transformation. This is not attributed to artefacts such as localised beam heating, as this would be expected to enhance one transformation whilst retarding the other. As stated above, the good agreement at which the peak temperature occurs in the austenite to ferrite transformation, as well as the lengths of the inverse and stagnant stages, indicates that interfacial conditions are sufficiently similar in both the TEM and dilatometry.

In hot stage TEM experiments, there is the potential for the acceleration of the kinetics due to diffusion along the surface of the thin foils. Laird and Aaronson [44], for example, found that this contributed to the development of atypical microstructures during θ phase precipitation in Al–Cu alloys. However, it should be noted that precipitation of this kind occurs on a different length scale: 10–100 nm, compared to the micrometer scale as in the present study. Conversely, Onink et al. [22] reported measured interface velocities for Fe-0.36 wt% C steels carried out using 120 kV and a 300 kV LaB_6 TEM microscopes (that is, with comparable microscope conditions to those described above). These measured velocities were comparable to calculated velocities. Therefore, from the most relevant results reported in the literature no significant acceleration of the kinetics is expected due to thin foil artefacts such as surface diffusion. The surface diffusion of Mn can be ruled out

during the stagnant stage, as any such artefact should have led to a reduction in the measured stagnant stage length.

The difference in velocities might also be related to the existence of a thermal gradient along the sample length during the dilatometry experiments on the order of 3 °C between the two thermocouples. As grains along the length of the specimen reach the peak velocity at different nominal temperatures, the peak velocity would be averaged out resulting in a lower overall estimate. Furthermore, the peak velocities were typically sustained for a relatively small time period and would have also been averaged out if measured over longer time intervals. Consequently, the disparity may be the result of the use of higher frequency measurements to precisely determine the temperature of the peak velocity. Over the entire cycle, the difference in the overall migration distance is a factor of ~2–3 (depending on assumed geometry), indicating that average velocities over the course of the cycle are closer than a comparison of the peak velocities might imply.

It is important to consider that there is also contribution from the assumed geometry of the specimen when calculating the migration distance from dilatometry data. Changing from spherical to cubic geometry increased the estimated migration distance by 3.4 μm. For this reason, the migration distance is not well defined when comparing the 3D dilatometry case with the 2-dimensional TEM observations (as well as the 1D modelling performed using DICTRA).

Van Leeuwen et al. [45] computationally compared the austenite to ferrite transformation kinetics for a given interface
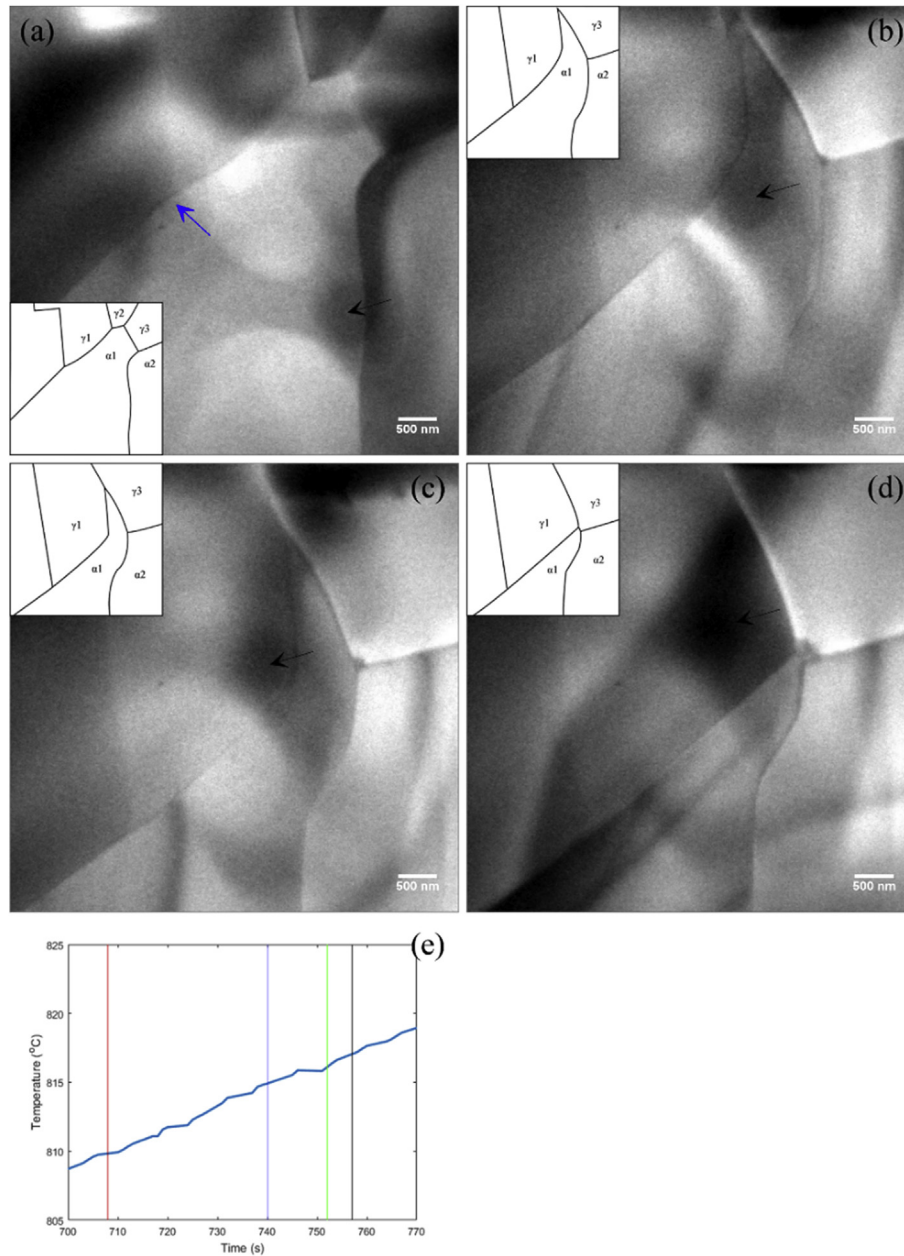
Fig. 7. Bright field TEM of the interface migration during the ferrite to austenite transformation (a) at 708.3 s (811 °C) (b) at 740.1 s (816 °C) (c) at 751.9 s (818 °C) (d) at 756.9 s (819 °C) and (e) Showing the time-temperature position of each frame. Vertical lines, from left to right, indicate the time depicted in frames (a)–(d). Black arrows indicate common positions between frames as the stage was moved.

mobility but by varying the number of nuclei per grain. The grain geometry was assumed to be a tetrakaidekahedron, which possesses grain edges and corners, unlike a spherical grain and so could incorporate more realistic nucleation. For a transformation which proceeds at constant velocity and with ferrite nucleating on each grain corner, a tetrakaidekahedron predicts a slower transformation than an equivalent spherical austenite grain. If fewer nuclei were assumed to form within the grain, the transformation rate became even slower.

In the present case, it is the rate of transformation that is fixed, and so by comparison with the model of Van Leeuwen et al. the spherical model would be expected to underestimate the migration velocity and distance. In the present study closer agreement, a factor of ~2, is achieved assuming cubic grain and edge nucleation as is assumed by Liu et al. [31,32] and Kempen et al. [34].

Dislocation movement was observed in the foils both during interface migration and in the period before migration began. Dislocations were most clearly visible on the ferrite side of the interface, although dislocations were also observed in the austenite. Periods of increased dislocation activity often corresponded with the austenite to ferrite transformation, indicating that the build-up of stress due to differences in specific volume between the two phases was potentially the cause of this activity. These dislocations moved towards the transformation interface before being eliminated. Similar behaviour was observed by Onink et al. [22] who suggested that with an appropriate Burgers vector and glide plane, dislocation movement could relax stresses. The observation of dislocations moving ahead of the interface and forming a new boundary in the ferrite was unique in the TEM observations. The process by which this occurs appears similar to
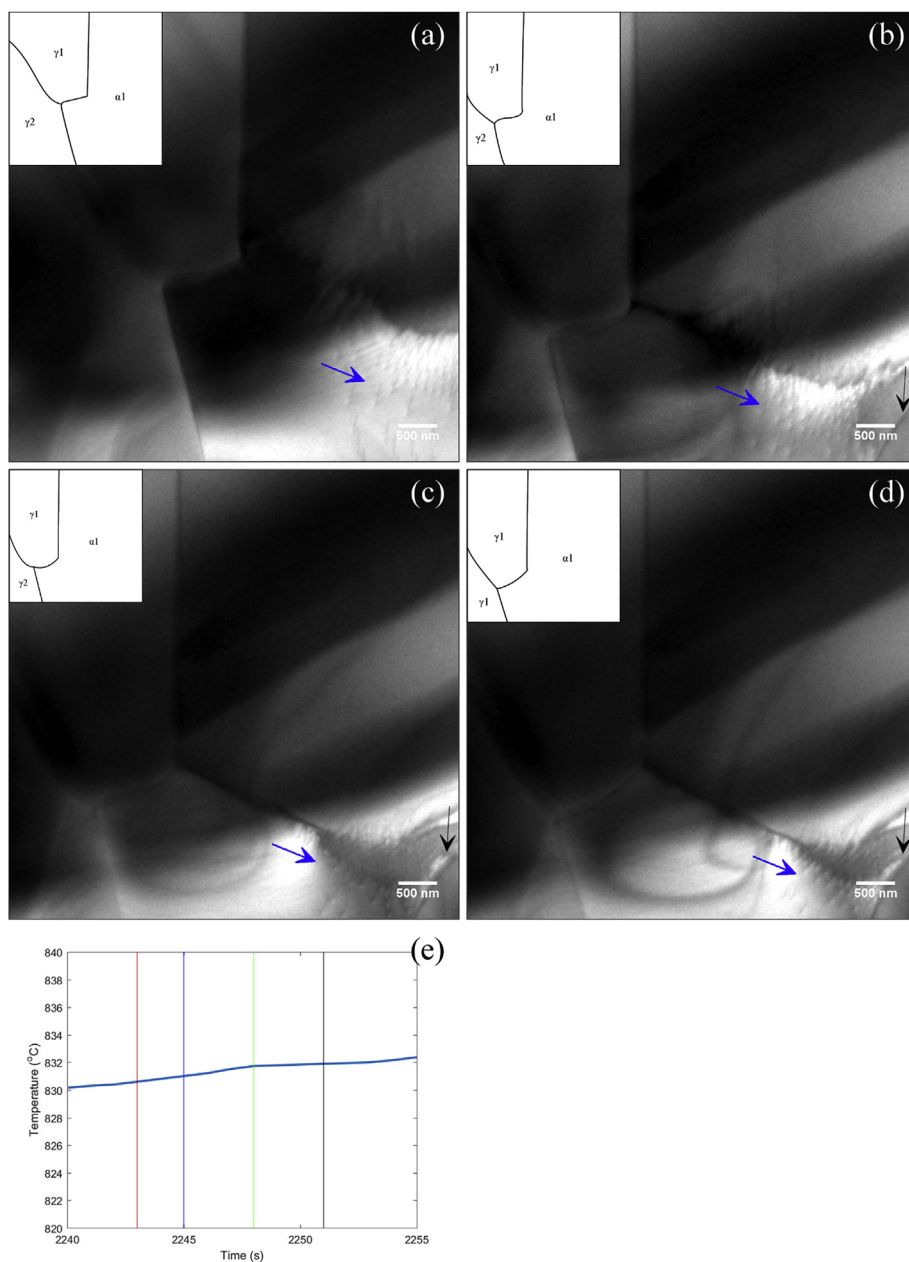
Fig. 8. Bright field TEM of the alignment of dislocations ahead of the moving interface during the ferrite to austenite transformation (a) at 2242.8 s (832 °C) (b) at 2244.8 s (832 °C) (c) at 2247.8 s (833 °C) (d) at 2250.7 s (833 °C) and (e) showing the time-temperature position of each. Vertical lines, from left to right, indicate the time depicted in frames (a)–(d). Black arrows indicate the position of an immobile ferrite grain boundary, blue arrows indicate a region with a high density of dislocations. (For interpretation of the references to colour in this figure legend, the reader is referred to the Web version of this article.)

traditional descriptions of recovery where large numbers of dislocations align to form low angle grain boundaries [46].

5. Conclusions

Successful cyclic partial phase transformation experiments were performed on a Fe-0.1C-0.5Mn alloy using hot stage TEM allowing the direct observation of the behaviour of individual austenite-ferrite interfaces. The interfaces were observed to display all the distinctive features of CPPT experiments including the normal and inverse transformations and a stagnant stage on both heating and cooling. There is a very good match in the stagnant stage length observed in the TEM, estimated to be 15–16 °C, and that predicted using kinetic modelling and found using dilatometry. This is approximately the expected length predicted from Chen et al. [15] when the different heating and cooling rates are considered.

There was no significant period during the stagnant stage during which the interface was completely static. Instead it was characterised by slow migration of the interface and a reversal in direction of that migration. However, total displacement over the course of the stagnant stage was less than 1 μm which would be undetectable in macroscopic dilatometric experiments. No special interface features were observed during the stagnant stage, but the interfaces became slightly straighter than during the faster transformation stages. During the fastest stages of transformation the interfaces showed some mode switching between straight and curved segmented growth.

There was a semi-quantitative agreement for the variation in

interface velocity during the non-stagnant stages of the transformation cycle with the velocities derived from dilatometric data. Peak velocities occurred at approximately the same temperatures and displayed the same overall behaviour. However, the TEM observations of the total distance migrated were a factor of 2 higher overall compared to the kinetic modelling or the first approximate made using dilatometry. This may be due to differences in assumptions about grain geometry and nuclei distribution.

Finally, the TEM observations showed several cases of strong acceleration of interface motion when two ferrite-austenite interfaces connected at a triple point came in closer contact. Clearly, in such cases minimisation of the total surface energy can provide an additional driving force for interface motion. Such an acceleration is not predicted by current phase transformation kinetic models but will have a minimal effect on the macroscopic transformation behaviour as only a very small volume fraction of the sample is affected.

Acknowledgement

Appendix A. Supplementary data

Supplementary data to this article can be found online at https://doi.org/10.1016/j.actamat.2019.07.047.

References

[1] H.K.D.H. Bhadeshia, R.W.K. Honeycombe, Steels: Microstructure and Properties, Butterworth-Heinemann, Amsterdam, 2006.
[2] M. Gouné, F. Danoix, J. Ågren, Y. Bréchet, C. Hutchinson, M. Militzer, G. Purdy, S. van Der Zwaag, H. Zurob, Overview of the current issues in austenite to ferrite transformation and the role of migrating interfaces therein for low alloyed steels, Mater. Sci. Eng. R (2015) 1–38.
[3] G. Purdy, J. Agren, A. Borgenstam, Y. Bréchet, M. Enomoto, T. Furuhara, E. Gamsjager, M. Gouné, M. Hillert, C. Hutchinson, M. Militzer, H. Zurob, ALEMI: a ten-year history of discussions of alloying-element interactions with migrating interfaces, Metall. Mater. Trans. A 42A (2011) 3703–3718.
[4] M. Hillert, L. Hoglund, Mobility of α/γ phase interfaces in Fe alloys, Scr. Mater. 54 (2006) 1259–1263.
[5] G.P. Krielaart, S. van der Zwaag, Kinetics of γ→α phase transformation in FeMn alloys containing low manganese, J. Mater. Sci. Technol. 14 (1998) 10–18.
[6] C.R. Hutchinson, H.S. Zurob, Y. Brechet, The growth of ferrite in Fe-C-X alloys: the role of thermodynamics, diffusion, and interfacial conditions, Metall. Mater. Trans. A 37A (2006) 1711–1720.
[7] H.I. Aaronson, W.T. Reynolds, G.R. Purdy, Coupled-solute drag effects on ferrite formation in Fe-C-X systems, Metall. Mater. Trans. A 35A (2004) 1187–1210.
[8] A. Phillion, H.S. Zurob, C.R. Hutchinson, H. Guo, D.V. Malakhov, J. Nakano, G.R. Purdy, Studies of the influence of alloying elements on the growth of ferrite from austenite under decarburization conditions: Fe-C-NI alloys, Metall. Mater. Trans. A 35A (2004) 1237–1242.
[9] J.W. Christian, The Theory of Transformations in Metals and Alloys: Part I, Elsevier Science Ltd, Oxford, 2002.
[10] C. Zener, Theory of growth of spherical precipitates from solid Solution, J. Appl. Phys. 20 (1949) 950–953.
[11] J. Sietsma, S. van der Zwaag, A concise model for mixed-mode phase transformations in the solid state, Acta Mater. 52 (2004) 4143–4152.
[12] H. Chen, S. van der Zwaag, An overview of the cyclic partial austenite-ferrite transformation concept and its potential, Metall. Mater. Trans. A 48 (2017) 2720–2729.
[13] H. Chen, B. Appolaire, S. van der Zwaag, Application of cyclic partial phase transformations for identifying kinetic transitions during solid-state phase transformations: experiments and modeling, Acta Mater. 59 (2011) 6751–6760.
[14] H. Chen, S. van der Zwaag, Application of the cyclic phase transformation concept for investigating growth kinetics of solid-state partitioning phase transformations, Comput. Mater. Sci. 49 (4) (2010) 801–813.
[15] H. Chen, M. Gouné, S. van der Zwaag, Analysis of the stagnant stage in diffusional phase transformation starting from austenite-ferrite mixtures, Comput. Mater. Sci. 55 (2012) 34–43.
[16] H. Farahani, H. Zurob, C.R. Hutchinson, S. van der Zwaag, Effect of C and N and their absence on the kinetics of austenite-ferrite phase transformations in Fe-0.5Mn alloy, Acta Mater. 150 (2018) 224–235.
[17] H. Chen, S. van der Zwaag, Indirect evidence for the existence of the Mn partitioning spike during the austenite to ferrite transformation, Philos. Mag. Lett. 92 (2) (2012) 86–92.
[18] H. Chen, S. van der Zwaag, Analysis of ferrite growth retardation induced by local Mn enrichment in austenite created by prior interface passages, Acta Mater. 61 (2013) 1338–1349.
[19] H. Chen, E. Gamsjaeger, S. Schider, H. Khanbareh, S. van der Zwaag, In situ observation of austenite-ferrite interface migration in a lean Mn steel during cyclic partial phase transformations, Acta Mater. 61 (2013) 2414–2424.
[20] H. Farahani, W. Xu, S. van der Zwaag, Determination of mode switching in cyclic partial phase transformation in Fe-0.1C-xMn alloys as a function of the Mn concentration, JOM (2019). https://doi.org/10.1007/s11837-018-03323-5.
[21] H. Fang, S. van der Zwaag, N.H. van Dijk, In situ 3D neutron depolarization study of the transformation kinetics and grain size evolution during cyclic partial austenite-ferrite phase transformations in Fe-C-Mn steels, Metall. Mater. Trans. A 49 (2018) 5962–5975.
[22] M. Onink, F.D. Tichelaar, C.M. Brakman, E.J. Mittemeijer, S. van der Zwaag, J. Mater. Sci. 30 (1995) 6223–6234.
[23] G.R. Purdy, The dynamics of transformation interfaces in steels-I. The ferrite-austenite interface in Fe-C-Mo alloys, Acta Metall. 26 (1978) 477–486.
[24] G.R. Purdy, On the direct observation of the formation of ferrite in steels, Scr. Metall. 21 (1987) 1035–1038.
[25] J. Du, F. Mompiou, W.-Z. Zhang, In-situ TEM study of dislocation emission associated with austenite growth, Scr. Mater. 145 (2018) 62–66.
[26] M. Nemoto, Growth of Bainite in an Iron-Nickel-Carbon Alloy in: High Voltage Electron Microscopy, Academic Press, London, 1974, pp. 230–234.
[27] M. Kang, M.-X. Zhang, M. Zhu, In situ observation of bainite growth during isothermal holding, Acta Mater. 54 (2006) 2121–2129.
[28] L.S. Darken, R.M. Fisher, Some Observations on the Growth of Pearlite in Decomposition of Austenite by Diffusional Processes, Interscience Publishers, New York, 1962, pp. 249–288.
[29] J. Nutter, Direct TEM Observation of the Movement of the Austenite-Ferrite Interface in Steels, PhD Thesis, University of Sheffield, 2018.
[30] J.O. Andersson, T. Helander, L. Hoglund, P.F. Shi, B. Sundman, Thermo-Calc and DICTRA, Computational tools for materials science, Calphad 26 (2002) 273–312.
[31] Y.C. Liu, F. Sommer, E.J. Mittemeijer, Kinetics of the abnormal austenite-ferrite transformation behaviour in substitutional Fe-based alloys, Acta Mater. 52 (2004) 2549–2560.
[32] Y. Liu, D. Wang, F. Sommer, E.J. Mittemeijer, Isothermal austenite-ferrite transformation of Fe-0.04 at.% C alloy: dilatometric measurement and kinetic analysis, Acta Mater. 56 (2008) 3833–3842.
[33] Y.C. Liu, F. Sommer, E.J. Mittemeijer, The austenite-ferrite transformation of ultralow-carbon Fe-C alloy; transition from diffusion- to interface-controlled growth, Acta Mater. 54 (2006) 3383–3393.
[34] A.T.W. Kempen, F. Sommer, E.J. Mittemeijer, The kinetics of the austenite–ferrite phase transformation of Fe-Mn: differential thermal analysis during cooling, Acta Mater. 50 (2002) 3545–3555.
[35] H. Farahani, G. Zijlstra, M.G. Mecozzi, V. Ocelík, J. Th. M. De Hosson, S. van der Zwaag, In Situ High-Temperature EBSD and 3D Phase Field Studies of the Austenite–Ferrite Transformation in a Medium Mn Steel, Microsc. Microanal. 25 (2019) 639–655.
[36] M. Furtkamp, G. Gottstein, D.A. Molodov, V.N. Semenov, L.S. Shvindlerman, Grain boundary migration in Fe-3.5% Si bicrystals with [001] tilt boundaries, Acta Mater. 46 (1998) 4103–4110.
[37] D.A. Molodov, U. Czubayko, G. Gottstein, L.S. Shvindlerman, On the effect of purity and orientation on grain boundary motion, Acta Mater. 46 (1998) 553–564.
[38] M. Hillert, Solute drag in grain boundary migration and phase transformations, Acta Mater. 52 (2004) 5289–5293.
[39] E. Schmidt, D. Soltesz, S. Roberts, A. Bednar, S. Sridhar, The austenite/ferrite front migration rate during heating of IF steel, ISIJ Int. 46 (2006) 1500–1509.
[40] M.A. Tschopp, K.N. Solanki, F. Gao, X. Sun, M.A. Khaleel, M.F. Horstemeyer, Probing grain boundary sink strength at the nanoscale: energetics and length scales of vacancy and interstitial absorption by grain boundaries in α-Fe, Phys. Rev. B Condens. Matter 85 (2012) 064108.
[41] N.R. Rhodes, M.A. Tschopp, K.N. Solanki, Quantifying the energetics and length scales of carbon segregation to α-Fe symmetric tilt grain boundaries using atomistic simulations, Model. Simul. Mater. Sci. Eng. 21 (2013) 035009.
[42] B.B. Vynokur, Influence of alloying on the free energy of austenitic grain boundaries in steel, Mater. Sci. 32 (1996) 448–455.
[43] Z. Yang, R.A. Johnson, An EAM simulation of the alpha-gamma iron interface, Model. Simul. Mater. Sci. Eng. 1 (1993) 707–716.
[44] C. Laird, H.I. Aaronson, Mechanisms of formation of θ and dissolution of θ' precipitates in an Al-4% Cu Alloy, Acta Metall. 14 (1966) 171–185.
[45] Y. van Leeuwen, S. Vooijs, J. Sietsma, S. van der Zwaag, The effect of geometrical assumptions in modeling solid state transformation kinetics, Metall. Mater. Trans. A 29 (1998) 2925–2931.
[46] F.J. Humphreys, M. Hatherly, Recrystallization and Related Annealing Phenomena, Pergamon, Oxford, 1996.